Coastal-Trapped Waves off the Coast of South Africa: Generation, Propagation and Current Structures

E. H. SCHUMANN

Institute for Coastal Research, Department of Oceanography, University of Port Elizabeth, Port Elizabeth, South Africa

K. H. BRINK

Woods Hole Oceanographic Institution, Woods Hole, Massachusetts

(Manuscript received 17 April 1989, in final form 7 February 1990)

ABSTRACT

Coastal sea level variations from six sites around South Africa are used to establish the characteristics of coastal-trapped wave (CTW) propagation. Substantial amplitudes (>50 cm) are found along the south coast, but further propagation on the east coast against the Agulhas Current is inhibited. Current measurements over the shelf in this region show barotropic reversals during the passage of the peak of a CTW, with essentially geostrophic flow occurring.

Comparisons are made with theoretically calculated first-mode CTW characteristics along various sections of the coast. These calculated speeds fall within the range of speeds determined from observation, though an admixture of a mode 2 CTW is possible. It is found that the speeds of wind systems moving along the coast also fall in the same range, probably leading to a resonance condition, and an explanation for the large CTW amplitudes.

1. Introduction

The existence of coastal-trapped waves (CTWs) with periods of a few days to weeks has been demonstrated along various coastlines around the world. Initial investigations used sea level measurements to identify the propagation of these signals, while later the associated current structures were also analyzed; LeBlond and Mysak (1978) list numerous such observations.

Identifications of CTWs have involved extensive arrays of temperature/current meters, sea level recorders and weather data to isolate their structure and propagation characteristics, although it was not until the Australian Coastal Experiment was carried out off New South Wales during 1983/84 that a specific search for CTWs was mounted (Freeland et al. 1986). Field studies have produced dramatic examples of these waves, for example the amplitudes (in coastal sea level) of more than 1 m reported off the south coast of Australia by Krause and Radok (1976). Models of CTWs include the effects of the alongshore component of the wind (often the prime generator of CTWs), as well as bottom friction, continuous stratification and realistic bottom topography (e.g., Chapman 1987).

Western boundary currents exert a dominant influence on adjacent coastal areas, and the evidence for the existence of CTWs in such regions (where they must propagate against the currents) has been far from conclusive. Analyses of data from the southeastern United States indicate that the lowest mode wind-forced CTW travels south in the Florida Straits (e.g., Brooks and Mooers 1977). In the south Atlantic Bight variations in coastal sea level are believed to be caused primarily by local wind (Schwing et al. 1985), although some evidence has been found for freely propagating waves during a transitional wind regime (Schwing et al. 1988).

There have been few investigations for CTWs off the coast of South Africa (Fig. 1). Gill and Schumann (1979) speculated on the existence of essentially internal CTWs, and came to the conclusion that the poleward flowing Agulhas Current would substantially inhibit their propagation. Schumann (1983) analyzed sea level data off the southeast coast, but found little evidence for such waves. De Cuevas et al. (1986) found that the propagation of sea level disturbances occurred down the west coast and along the south coast, but that this did not continue through to Durban on a regular basis. More recently Jury et al. (1989) have analyzed specific cases of propagating sea level disturbances associated with weather systems.

In 1984 experiments were conducted off East London (Fig. 1) using both moorings and routine ship measurements. The shelf is relatively narrow in this

Corresponding author address: Dr. Eckart Schumann, Department of Oceanography, University of Port Elizabeth, Box 1600, Port Elizabeth, South Africa.

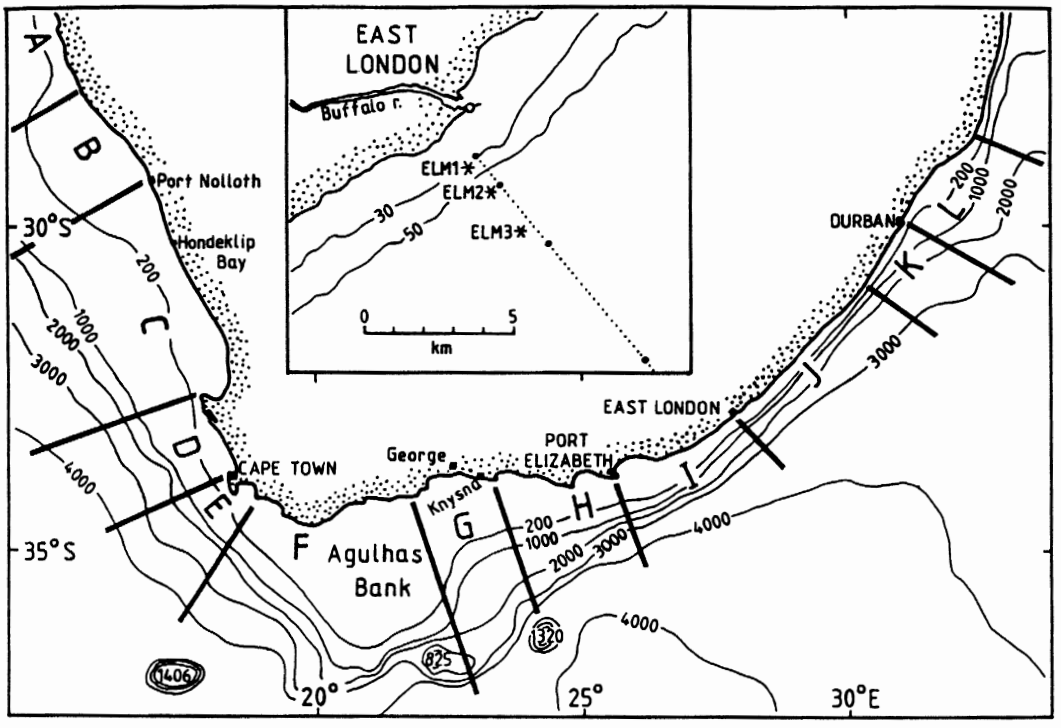

FIG. 1. The Southern African coastline showing bathymetry and the various sites referenced in the text; the sections of coast identified in the theoretical CTW determinations are shown. The inset map gives details of the measurement localities at East London: the weather station is shown by an open circle on the south breakwater, the mooring positions are shown by asterisks, and the first four ship stations (solid circles) on the offshore line are also indicated.

area, with the 200 m isobaths only about 23 km from shore, and a dominant southwestward flow associated with the Agulhas Current even closer to the coast (Schumann 1987). However, fairly regular current reversals occur, and the existence of CTWs is further investigated here in an attempt to account for these variations. Coastal sea level at other sites is incorporated, as well as forcing by the alongshore wind; the results presented confirm that substantial CTWs do occur, particularly along the south coast.

2. The measurements

An ocean measurement program involving ship stations and moorings was carried out off East London over a period of about nine months in 1984 (Fig. 1). The data used here come from the line of ten stations extending 50 km off East London itself, as well as from the three mooring positions shown.

Four cruises, using the CSIR's R/V *Meiring Naude*, were undertaken in April, June, September and November. All the stations were worked on the first two cruises, but inclement weather in September meant that only eight of the ten stations on the East London line could be completed. In November instrumentation problems resulted in only seven stations on the line being completed.

A Neil Brown CTD was used exclusively on the first two cruises, giving temperature with an accuracy of 0.01°C, and salinity with an accuracy of 0.001. A CSIR-built hydrosonde, which measured current and temperature and took water samples for salinity determinations, was used on the third and fourth cruises. Temperature accuracy is 0.05°C, while current speed and direction accuracy depends on the position-fixing accuracy of the ship; results shown here are considered to have an accuracy better than 15 cm s^{-1} and 15°.

The depth falls off quickly at the mooring positions, and a single current meter was deployed on the inshore mooring ELM1 about 1.3 km offshore in 30 m depth, two meters on ELM2 at 2.4 km offshore in 65 m of water and also two meters on ELM3 about 4.1 km offshore in 80 m. They were positioned this close to the coast because of the known strong flows associated with the Agulhas Current (Harris 1978), and it was not certain how the moorings would cope. There were two main experimental periods when these moorings were deployed, namely between the first and second cruises, and then again between the third and fourth cruises; the mooring at the inshore site ELM1 was maintained over the whole period of the measurements. Additional moorings were deployed five and ten kilometers north of ELM1 and ELM3 respectively, but the results are not reported here because of a limited

data return and similarity with the more southern moorings.

Aanderaa RCM4 meters were used for all moored temperature/current measurements and were set to record at 15 minute intervals. Where water depth allowed, the topmost meter was situated at a depth greater than 30 m with subsurface buoys in order to minimize the effect of surface waves and rotor pumping (Halpern and Pillsbury 1976). There was a reasonably good data return, with loss of some data due to faulty equipment and mooring problems. During the first experimental period in April to June good current data were obtained at all the three sites ELM1, ELM2 and ELM3, though the encoder malfunctioned at the bottom meter at ELM2 before the end of the deployment. A meter recording hourly values was deployed at ELM1 in August, but by the time of the second experimental period in September and October growth had fouled the rotor and vane.

An Aanderaa automatic weather station was erected on the south breakwater of the harbor a few weeks before the first cruise: this site is relatively flat, suitably removed from the effects of buildings, and within the coastal environment. The variables measured by the weather station of relevance here are wind speed (accuracy 2 percent or 20 cm s^{-1}), wind direction (accuracy 5°) and air pressure (accuracy 0.2 mb). Two days of data were missed in September when magnetic tape in the recorder ran out, and 22 days of wind data were lost in October/November when the anemometer stopped working. Measurements were recorded at 15 minute intervals.

Additional data are available from other sites along this coast. Sea level is measured to an accuracy of 1 cm at all the major harbors, and hourly data were obtained for Port Nolloth, Cape Town, Knysna, Port Elizabeth, East London and Durban, covering a coastline of almost 2000 km. Meteorological variables are also measured at the airports at Cape Town, George, Port Elizabeth and Durban: wind speed to an accuracy of 0.1 m s^{-1} and direction to within 10°. Air pressure measurements at the airports are to an accuracy of 0.1 mb, with additional data from a station near Hondelklip Bay operated by the Sea Fisheries Research Institute. Although there are recognized shortcomings in these data because of variations at the land/sea interface (Hunter 1982) and the position of the airports away from the coast, they are nonetheless useful for determining the propagation of weather systems, for adjusting sea level and for investigating the generation of CTWs. Data were obtained for an approximate nine-month period starting in March 1984. Table 1 gives details of what was available at the different sites; short, intermediate breaks were interpolated, but the weather data did span both intensive ocean experimental periods.

The 15-minute time series values were filtered using a Cosine-Lanczos filter with 24 weights and a half-power point at 0.5 cycles/hour, and decimated to hourly values. Since the periods of interest fall in the "weather band," i.e. several days and longer, all hourly values were then subjected to a further Cosine-Lanczos filter with 97 weights and a half-power point of 40 hours, and decimated to 12-hourly values.

3. CTW propagation

Sea level data can be used to investigate CTW propagation. However, in order to obtain the actual pressure variations in the ocean associated with CTWs, it is important to adjust the measured sea level for air pressure variations. Thus, if p_a is the air pressure variation in mb, the adjusted sea level is given by η, where

$$\eta = 0.99 p_a + \eta_0 \qquad (1)$$

and η_0 is the actual measured sea level.

For the analysis performed here it is the adjusted sea level which will be used, and unless otherwise stated any reference to sea level will specifically mean adjusted

TABLE 1. Data site spacing relative to Port Nolloth: the distances have been estimated approximately by measuring along a smoothed coastline. The sea level and meteorological data available for each of the sites is given; where two values are given (PE and EL), the first refers to air pressure, and the second to wind. The total range and standard deviation in sea level has been determined for the low frequency filtered data, i.e. tides are excluded. The principal axes (Pr ax) directions have been determined for the wind, and are given in terms of the westerly component (Schumann 1989).

		Sea level			Meteorology	
Site	Position (km)	Data (days)	Range (cm)	Std dev (cm)	Data (days)	Pr ax (°T)
Port Nolloth (PN)	0	259	49	7.5		
Hondeklip Bay (HB)	120				280	
Cape Town (CT)	530	267	49	7.5	275	346
George (Ge)	970				275	277
Knysna (Kn)	1020	267	93	12.6		
Port Elizabeth (PE)	1250	267	73	12.7	228–275	246
East London (EL)	1490	217	79	14.6	253–203	225
Durban (Db)	1950	249	56	9.5	275	209

sea level. For adjusting sea level at Port Nolloth and Knysna the closest air pressure values available were those from Hondeklip Bay and George, respectively; for the other four sites sea level and air pressure were measured in the same locality.

A preliminary statistical analysis was performed on the low frequency, 12-hourly values of sea level at the various sites, and the results are given in Table 1. It is clear that there are substantial variations in sea level occurring, with ranges of one-half meter and more at most sites. The variability around the coast is also of considerable interest, with both the range and standard deviation smallest off the west coast, with values half of those on the south coast. At Durban the variability is again decreased.

Figure 2 shows space–time contours for sea level covering the periods of the two intensive experiments. The characteristics portrayed in the results in Table 1 also appear, namely the extent of the variability in sea level along the south coast stations. The propagation of this variability from west coast to east coast sites is also apparent, as would be expected from CTWs. However, on many occasions propagation is not continuous from Port Nolloth to Cape Town, while there is an even more abrupt drop in amplitude between East London and Durban. While it is difficult to arrive at a general propagation speed of the "events," rough calculations of the more prominent occasions give a range between 4.2 and 6.7 m s^{-1} (360 to 580 km day^{-1}).

Autospectra of sea level are shown in Fig. 3, with clear differences between the west, south and east coasts; the analysis of de Cuevas et al. (1986) also shows changes in going from the west to south coasts. At Port Nolloth there is a relatively flat spectrum with lower energy at longer periods than at the other sites. At Cape Town a clear wide peak at a period between 10 and 15 days emerges with a rapid drop-off at shorter periods.

The approximately 10-day peak is amplified considerably at Knysna and Port Elizabeth, and maintains the same peak energy at East London. There is some indication of the development of 5-day and 3.5-day peaks along the south coast, reflecting the close coherence between the three sites also seen in Fig. 2. The Durban spectrum is markedly different, being dominated by long period energy with little correlation in the peaks with the southern sites. The emergence of substantial energy at long periods at the south and east coast sites is possibly related to variations in the Agulhas Current.

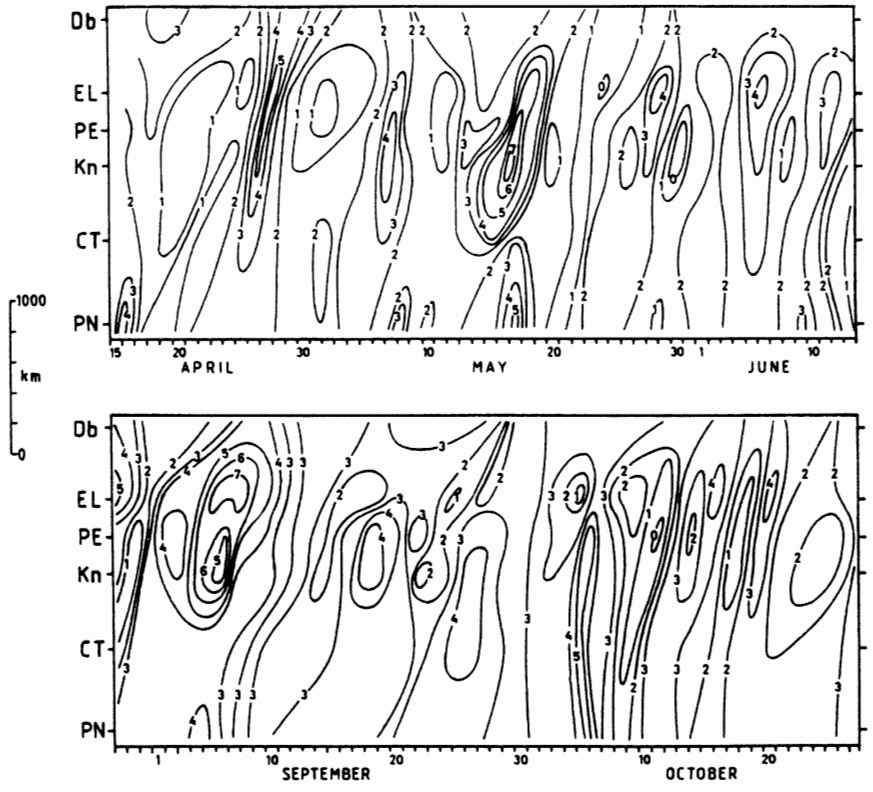

FIG. 2. Space–time contours of sea level covering the periods of the two intensive experiments. The positions of the various sites are given on the space axis (abbreviations as in Table 1), while the relevant dates are given on the time axis. The filtered sea level records were demeaned, and then adjusted so that the lowest contour corresponded to zero; contour units are in 10 cm intervals.

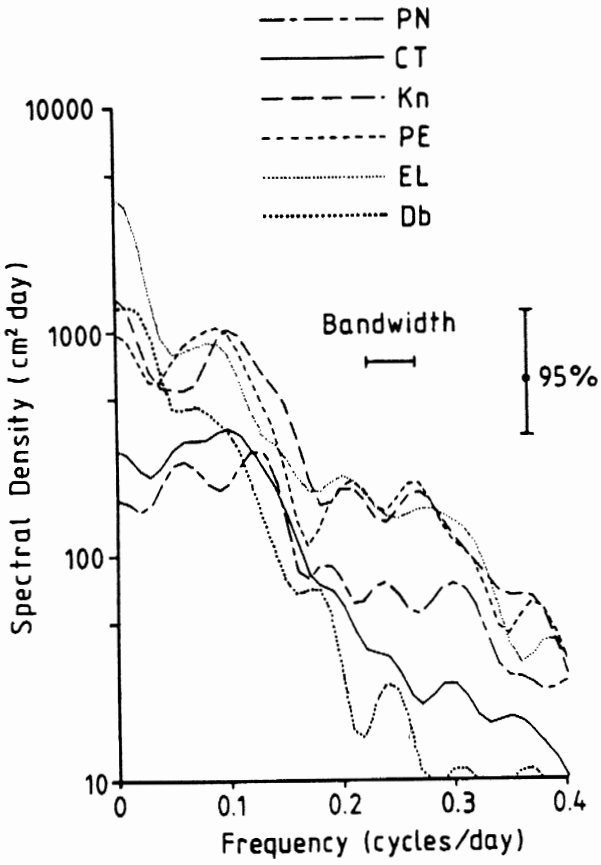

FIG. 3. Autospectra of sea level from the various sites. The given bandwidth is the same for all spectra, but the 95% confidence limit shown varies slightly because of the different lengths of the series.

Alongshore coherence and propagation of this sea level variability is investigated further in Fig. 4. On the west coast a significant coherence is found at a period of about 14 days; de Cuevas et al. (1986) also found such a peak for this section of coast. Of interest is the fact that this peak again appears on the east coast from Port Elizabeth to East London and to a lesser extent East London to Durban. It is not clear why these peaks should emerge, but could be due to local forcing from propagating wind systems that are not as significant along the south coast; Schumann (1983) found a propagating signal in the Durban region that apparently did not originate farther south.

The peak broadens from Cape Town eastwards along the south coast, until between Port Elizabeth and East London high coherency is found for periods ranging from 3 to 20 days; the closer spacing of the south coast sites will obviously contribute to the higher coherency. For all these peaks the phase is such as to represent propagation from west to east, and some of the peaks are identified in Table 2 together with the range of propagation speeds associated with 95% confidence limits for the phase. The speeds all fall within the bounds expected for CTWs, with a maximum along the south coast.

Halliwell and Allen (1984) first used joint space- and time-lagged correlations to analyze the propagation of CTWs along the Pacific coast of North America. Figure 5 shows similar correlations of sea level at all the sites relative to sea level at Port Elizabeth and East London. The features of Fig. 2 again appear, in particular the development of sea level propagation from Cape Town through to East London, and the disappearance of the signal before reaching Durban. Of further note is the broadening of the correlation peak at East London in Fig. 5b; meaning that a higher autocorrelation exists for a longer period, i.e. the spectrum is redder.

Figure 5 can also be used to determine speeds of sea level propagation, using the slope of the line through

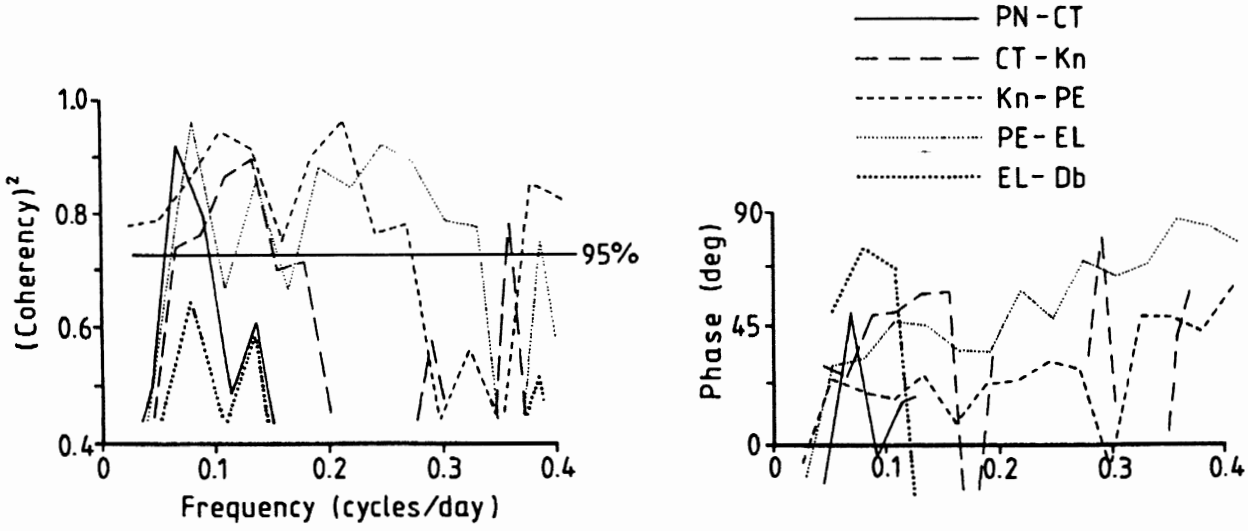

FIG. 4. Coherency squared and phase spectra of sea level for adjacent sites. The 95% confidence limit is shown, with the phase then also drawn only for higher values of coherency. The phase is positive if the first-named site leads.

TABLE 2. Identified peak periods in the sea level and principal axis wind component coherency spectra of Figs. 4 and 8. The associated propagation speeds of CTWs and wind systems have been determined from the phase spectra, the range being due to the 95% confidence limits.

	Sea level		Wind	
Coastal section	Period (days)	Speed range (m s^{-1})	Period (days)	Speed range (m s^{-1})
PN-CT	14.8	2.7–3.0		
CT-Kn	7.5	4.4–5.0		
CT-Ge			15.3	2.1–4.6
			6.4	3.3–5.1
Kn-PE	9.4	5.1–6.9		
	4.6	7.7–9.1		
Ge-PE			15.3	2.8–8.1
			7.5	3.4–11.8
			4.5	5.8–20.3
			3.4	5.1–9.1
PE-EL	12.4	2.3–2.6	11.8	4.7–6.0
	7.3	2.6–3.7	5.7	3.6–8.6
	4.0	4.9–5.5	3.7	6.3–7.3
EL-Db	12.4	1.6–2.7	5.7	8.5–10.6
			3.3	8.4–14.2

the maximum correlation at each distance position. With such a few measurement sites, this line has been drawn in by eye, and it is apparent that that speed varies along the coast; in particular in Fig. 5a there is also a decrease in speed beyond Port Elizabeth. The average speed along the south coast is determined to be about 4.9 m s^{-1} (420 km day^{-1}), but an increase in the Knysna–Port Elizabeth region of up to 6.5 m s^{-1} (560 km day^{-1}); this agrees with the result from Fig. 2 and falls within the ranges given in Table 2. These propagation speed estimates from lagged correlations between sea level records represent the joint effects of wind driving and of free wave propagation (Allen and Denbo 1984). For this reason, such speed estimates can be expected to differ from that of the free CTWs in isolation.

The lack of coherence between East London and Durban is a confirmation of the results of Schumann (1983). It is clear that most of the time CTWs do not propagate northeastwards against the Agulhas Current, and Brink (1990) has given an explanation for this in terms of increased damping due to the tendency of a mean flow (here the Agulhas Current) to distort the free wave modal structure so that wave currents are strongest where the water is shallowest. Even at the long period end there is little coherence, possibly a result of the inshore gyre off Durban described by Schumann (1982), so that there is only a limited influence of the Agulhas Current at the measuring site in the Durban harbor.

The theoretical propagation characteristics of long, free, lowest mode CTWs can be determined from known topography, latitude and stratification using the programs in Brink and Chapman (1987). The results, summarized in Table 3, show that the waves propagate very rapidly around South Africa (phase speed $c > 6$ m s^{-1}) except along the east coast (sections I, J, K and L in Fig. 1) where the shelf is rather narrow. There are likely to be differences between these calculated values and the experimental results since the CTWs measured in the ocean are expected to be multimode signals. The calculations including stratification yield kinetic/potential energy ratios R that are large where the shelf is wide, indicating behavior similar to barotropic continental shelf waves. Indeed, in these cases the barotropic and stratified results are similar. In the narrow shelf regions, R is closer to unity suggesting behavior more akin to internal Kelvin waves. In all cases, stratification acted to increase phase speed. Also included are estimates of the e-folding time for decay due to bottom friction, T_f, estimated using the bottom resistance coefficient of 0.05 cm s^{-1} and the method of Brink (1990).

In the region where the Agulhas Current comes particularly close to the shore (sections I, J and K) barotropic modal calculations were also made which include a mean alongshore flow which peaks at 1.55 m s^{-1} at the 200 m isobath (Pearce 1977). In these cases the propagation speed decreases somewhat relative to the barotropic case with no mean flow. Frictional decay distances are decreased by adding a mean flow, especially for sections I and K. Thus the Agulhas is not strong enough to 'reverse' the direction of CTW propagation, but its enhancement of wave damping is dramatic.

The calculated free wave speeds suggest that lowest mode waves should propagate from Cape Town to Port Elizabeth at speeds ranging from 5 to 13 m s^{-1} for the barotropic situation, and between 6 and 14 m s^{-1} in stratified conditions, with the highest speeds in the wide Agulhas Bank area. Note that even though intense thermoclines occur on the Agulhas Bank in summer, and are broken down in winter (Schumann and Beek-

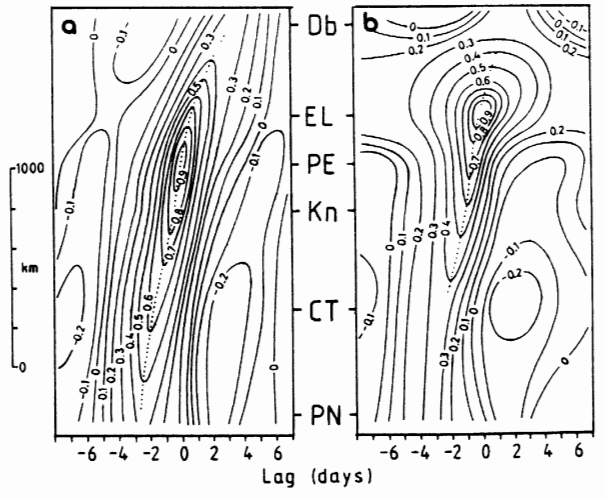

FIG. 5. Normalized time-lagged cross-correlations between sea level measured at the various sites on the ordinate axis, and sea level at (a) Port Elizabeth and (b) East London.

TABLE 3. Properties of the first mode modelled free CTW's for the sections identified in Figure 1; c is the calculated CTW speed, T_f the e-folding frictional decay time, and R the kinetic/potential energy ratio. In parentheses in the wave speed column are given the corresponding wave speeds of the second mode wave.

	Stratified			Barotropic No mean flow		Barotropic with mean flow	
Section	c (m s^{-1})	T_f(days)	R	c (m s^{-1})	T_f(days)	c (m s^{-1})	T_f(days)
A	6.32 (3.00)	6.6	8.1	5.00 (2.24)	5.6	—	—
B	8.32 (4.52)	4.0	11.1	7.30 (3.61)	3.6	—	—
C	12.10 (4.74)	8.3	16.6	10.77 (3.88)	7.9	—	—
D	6.50 (2.83)	8.4	8.3	5.10 (2.11)	7.3	—	—
E	6.14 (3.42)	4.6	8.8	5.07 (2.84)	3.8	—	—
F	14.10 (3.12)	2.8	8.3	13.29 (2.27)	2.7	—	—
G	10.02 (5.52)	5.0	11.9	9.30 (4.80)	4.6	—	—
H	7.46 (3.66)	4.8	8.6	6.37 (2.70)	4.2	—	—
I	4.20 (2.39)	5.3	4.3	2.77 (1.44)	3.0	2.17	1.8
J	3.41 (2.10)	19.5	4.3	2.22 (0.99)	27.3	1.55	3.5
K	2.72 (1.00)	18.9	2.1	1.34 (0.67)	17.5	0.65	3.8
L	4.95 (2.53)	10.7	8.0	3.93 (1.70)	10.3	—	—

man 1984), the speed of the baroclinic CTWs depends essentially on the surface to abyssal density difference, and therefore do not change much on a seasonal basis. These calculated speeds are at the upper limit of the speeds determined in Table 2, and the range of between 4.2 and 6.7 m s^{-1} derived from Figs. 2 and 5. On the other hand, the observed speeds fall in the upper limits of the calculated second mode CTW speeds in this region (Table 3).

In section 5, the issue of the theoretical versus observed propagation speeds will be resolved. However, the relationship between currents and sea level near East London will first be addressed in order to test its consistency with CTW theory.

4. Ocean structures at East London

Offshore temperature sections on the East London line are shown in Fig. 6. Some seasonal variations are evident, with the establishment of a fairly weak thermocline in autumn (April) and spring (November). The sloping isotherms beyond the shelf break are indicative of the presence of the Agulhas Current (Pearce 1977). The near-surface currents shown confirm this conclusion, with substantial speeds beyond the shelf break; the instantaneous value of 2.7 m s^{-1} measured on the September cruise is one of the highest values recorded in the Agulhas Current. There was little variation of current strength with depth over the shelf, and

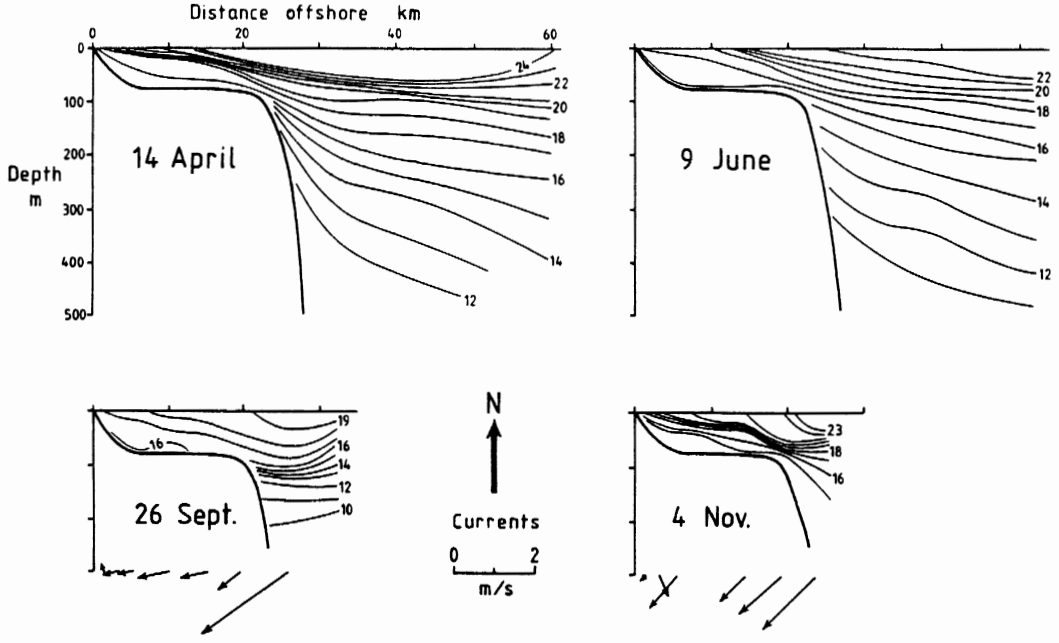

FIG. 6. Temperature sections made offshore on the East London line on the four cruises in 1984. Current measurements were also made on the September and November cruises, and the currents at 10 m depth are shown.

the influence of the Agulhas Current can be seen right up to where more abrupt shoaling occurs at the coast.

Clarke and Brink (1985) have given a criterion for barotropic shelf water response to wind forcing, namely

$$N^2\alpha^2 f^{-2} \ll 1 \qquad (2)$$

where N is a shelf-averaged value of the buoyancy frequency, α is an averaged bottom slope and f is the Coriolis parameter. A more restrictive case occurs when $N\alpha f^{-1} \ll 1$, and under these conditions almost all the wind-driven fluctuations can be expected to be confined to the shelf area.

Assuming minimal changes in salinity (justified by Pearce 1977), the temperature sections shown in Fig. 4 can be used to calculate the criterion in (2), outside of the coastal boundary layer. Values range from 0.01 in winter to 0.9 in summer, indicating that marked seasonal varations from barotropic to baroclinic could occur. In either case most of the fluctuations should occur on the shelf, partly because of the barotropic flow, but also because of the effect of the Agulhas Current (Brink 1990).

Mitchum and Clarke (1986) established that, for wind forcing, the coastal boundary occurs effectively at a distance b from the coast at a depth of about three times the Ekman layer e-folding scale; within this frictional dynamics region the surface and bottom Ekman layers interact. Because of the variability of the coefficient of vertical eddy viscosity it is difficult to ascertain the precise value of this scale, but it is likely to be of the order of 40 m (e.g., Mitchum and Clarke used a value of 26 m on the west Florida shelf). With the rapid dropoff of topography at the coast the meters at positions ELM2 and ELM3 should have been outside this boundary layer, but with ELM1 near to b.

Figure 7 shows results from the experimental periods April–June and September–October 1984. The correspondence between marked changes in sea level—ranging between 25 and 50 cm—and current reversals is clear; the peaks in the sea level variations also correspond with propagating peaks clearly shown in Fig. 2. In the first experiment a regular periodicity of about ten days is evident, while a shorter period, lower amplitude fluctuation occurred during the second; the associated current reversals are evidently barotropic, in accord with the calculated regression coefficients. The available East London wind is also shown; however, there is no evident and consistent relation with local sea level or currents, particularly in deeper water.

The flow is essentially parallel to the coast, and principal axis directions can be determined using the technique described by Kundu and Allen (1976). These results are shown in Table 4, and a difference of about seven degrees is evident between the two series; it is not clear what caused this, since it is unlikely to be equipment error with such a consistent variation at all

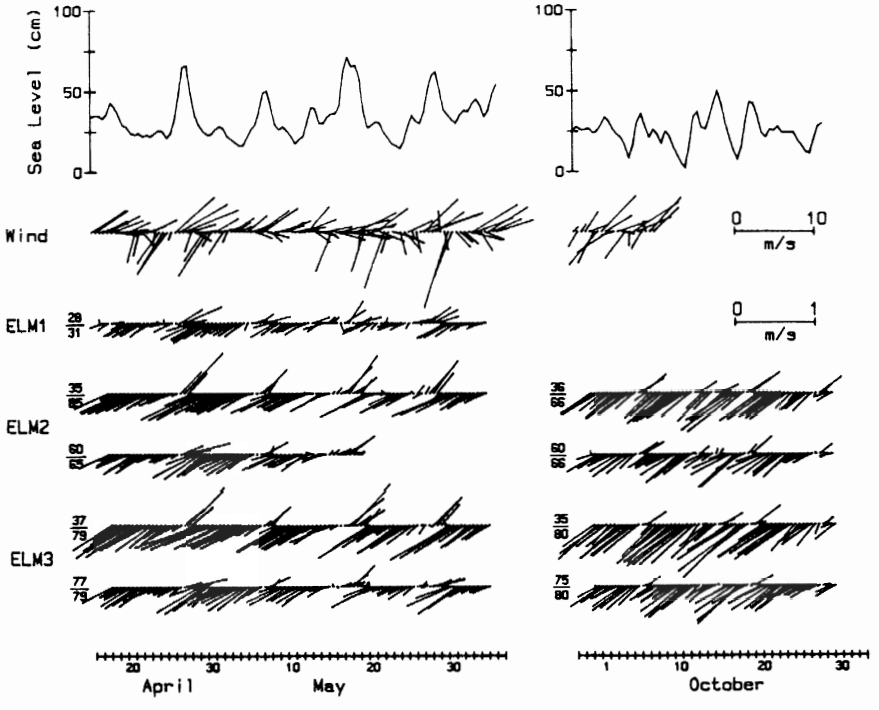

FIG. 7. Filtered, 12-hourly time series of sea level, wind and currents made off East London during the two intensive experiment periods; the orientation of the vectors is such that north is to the top of the page. The mooring sites are labeled (see Fig. 1), while the numbers on the left give the depth of the meter and the total water depth, e.g. 35/65 means the meter was at 35 m in 65 m of water.

the moorings. As expected, the mean current is southwestward with the Agulhas Current, and slower values are found near the sea bed. The veering at the bottom reported by Schumann (1987) is also apparent.

Coastal sea level variation should usually be dominated by the first-mode CTW (Clarke and Van Gorder 1986). For long CTWs the alongshore flow can be assumed to be in geostrophic balance with the offshore pressure gradient (LeBlond and Mysak 1978) and an estimate can be made of the sea level variations required for the magnitude of current reversals measured. Thus, for a coordinate system where the y-axis points along the coastline, with the x-axis offshore, geostrophy implies:

$$fv = g\frac{\delta\eta}{\delta x} \tag{3}$$

where v is the y-component of velocity, g is the acceleration due to gravity, and $\delta\eta$ is the change in adjusted sea level over the length scale δx.

Geostrophy (3) implies a linear relationship between alongshore current variation v and changes in coastal sea level $\delta\eta$. A regression analysis was done between v and η, and the results are also given in Table 4. The correlation coefficients are all high enough for some confidence to be placed in the geostrophic relation (3), and an approximately constant value for δx. It is also apparent that the regression coefficient is consistently higher for the topmost meters at ELM2 and ELM3 compared with the bottom meters, indicating a greater current response for a given change in coastal sea level; this could be due to frictional effects in the bottom boundary layer. The regression coefficient also increases with distance offshore. It is not clear why this should be, although weaker fluctuations can be anticipated in water shallower than 40 m because of bottom friction. Models which include the Agulhas (Brink 1990) do not have such an offshore increase in amplitude. An average value for the regression coefficient for all the meters is 1.8 s^{-1}. This value implies that a change of sea level of 50 cm is associated with a change of current speed of 90 cm s^{-1}, which certainly agrees with a visual inspection of Fig. 7.

TABLE 4. Principal axis (Pr ax) directions for the current measurements made at the specified sites during the two experimental periods (a) April to June, and (b) September and October. The meter depths over the water depths are given in brackets, while the current value given is the mean value along the principal axis direction; positive indicates flow in a southwestwards direction. Results of the regression analysis with local sea level are also given.

Mooring	Pr ax (°T)	Current (cm s^{-1})	Regression coefficient (s^{-1})	Correlation coefficient
		(a) Apr to Jun		
ELM1 (28/31)	243.9	11	1.21	0.68
ELM2 (35/65)	242.3	26	1.92	0.76
ELM2 (60/65)	244.4	21	1.52	0.79
ELM3 (37/79)	240.6	34	2.26	0.80
ELM3 (77/79)	242.4	23	1.43	0.73
		(b) Sep and Oct		
ELM2 (36/66)	234.6	32	2.12	0.66
ELM2 (60/66)	237.8	27	1.60	0.67
ELM3 (35/80)	233.7	45	2.53	0.73
ELM3 (75/80)	235.8	33	1.68	0.72

The results of the regression analysis can be related to the results of CTW theory. Specifically, the baroclinic CTW first mode structure for section J (Fig. 1, Table 3), can be used to predict the ratio between coastal sea level and currents. The model predicts that the regression coefficient should be 2.8 s^{-1} on the 66 m isobath and 2.7 s^{-1} on the 80 m isobath. There is little depth variation in these values since alongshore currents only vary in the vertical by 2% on the 80 m isobath and even less inshore. The velocity–sea level regression at the shallower meter at ELM3 (2.3–2.5 s^{-1}) agrees fairly well with the model value of 2.7–2.8 s^{-1}. Near-bottom values may not be expected to be in good agreement because of bottom boundary layer effects. A barotropic model predicts regression coefficients of 4.3–4.4 over the shelf, and a barotropic model including a mean flow (Agulhas) predicts values of 8–12. Clearly the stratified model fits best.

The model–observation agreement becomes poorer closer to the shore, which may be an indication of enhanced frictional effects. Alternatively, the presence of more than one CTW mode or of a non-wave component could also account for the discrepancy. In summary, though, the ELM3 current–sea level regressions, at least, are consistent with the presence of a lowest-mode CTW.

The smaller regression coefficient at ELM1 in April to June is possibly due to the position of the meter so close to the coast, and thus within the frictional dynamics region $x < b$; from Fig. 1 this is a very narrow region, probably less than 2 km wide. Mitchum and Clarke (1986) show that there is a rapid increase in wind-driven alongshore velocity from zero at the coast to a local maximum within $x < b$. The similarity in the response at ELM2 and ELM3 (Fig. 7 and Table 4) would seem to indicate that the boundary was near to or within the middle mooring position ELM2; this is also some justification in using the value of 40 m for the depth at the boundary.

5. CTW generation

While evidence has been presented for the propagation of CTWs along the coast of South Africa, particularly along the south coast, their generation remains to be investigated. Such waves are generally forced by the weather, and in particular the alongshore component of the wind (e.g. LeBlond and Mysak 1978). In order to consider such wind-generation of CTWs a brief understanding of the weather patterns over South Africa is necessary.

These weather patterns are dominated by two semi-permanent high pressure systems over the south Atlantic and southwest Indian oceans (Hunter 1987). The centers of these anticyclone systems move through about 6° of latitude from winter to summer (Preston-Whyte and Tyson 1988), resulting in markedly different seasonal wind regimes, particularly in the southwest Cape (Nelson and Hutchings 1983). In summer the south Atlantic high ridges eastward predominantly south of the continent, and the associated frontal systems also generally miss the land; in winter the systems often pass over the southern part of the subcontinent. Associated with the fronts are shallow low pressure systems, termed "coastal lows," which propagate in an anticlockwise sense around southern Africa; Gill (1977) modelled these in terms of CTWs in the atmosphere against the interior escarpment.

At all times the weather systems propagate from west to east (Schumann 1989), in particular the aforementioned coastal lows. With the short time series available here, no distinction will be made between summer and winter, and the analysis will use all the data. While it is likely that different peak periods existed at different times (e.g., see Figs. 2 and 7), such periods should nonetheless emerge if they are important.

For the generation of CTWs in the ocean it is possible for a condition of resonance to exist, i.e. if the speed of the generating wind systems matches that of the CTWs, then large amplitude waves can build up. However, analyses to date using air pressure measurements have shown that the coastal lows generally move much faster than the CTWs: Preston-Whyte and Tyson (1973) found values ranging from 5.5 to 14.6 m s^{-1}, the theoretical estimate of Gill (1977) was 20 m s^{-1}, while Schumann (1983) found a value of 29 m s^{-1} between Port Elizabeth and Durban.

Schumann (1989) analyzed the propagation of air pressure and wind systems along the coast of South Africa using data for the same period as that reported here. An unexpected result was the relatively low coherence between air pressure variability at the different sites and the local alongshore wind components. In addition, the propagation speed of the wind systems was considerably slower than the air pressure systems. In analyzing the generation of CTWs here, only the alongshore wind will be considered. Principal axes were determined for the wind using the same technique as for currents, with the directions at the different sites given in Table 1; it is clear that the major axes follow the orientation of the coastline.

In Fig. 8 the time-lagged cross-correlations of the major axis wind components at Port Elizabeth and East London with those at the other sites have been calculated. The slope of the line joining points of maximum correlation (determined by eye) varies with position, indicating different speeds. The limited number of measurement sites is an obvious drawback for precise determinations in this case, but an approximate speed along the south coast is 7.4 m s^{-1} (640 km day^{-1}). In

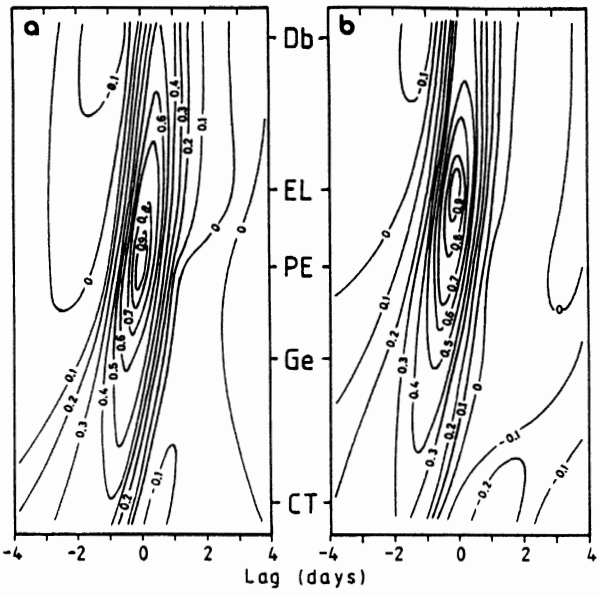

FIG. 8. Normalized time-lagged cross-correlations between the principal axis component winds at the various sites given on the ordinate axis, and the corresponding wind at (a) Port Elizabeth, and (b) East London.

contrast, Schumann (1989) found that the air pressure systems propagated at about 19 m s^{-1} (1600 km day^{-1}).

To investigate this further, Fig. 9 shows coherency and phase spectra for the major wind axis components considering adjacent sites around the coast; in Table 2 are also given the identified peak periods and range of propagation speeds. There is generally low coherence between Cape Town and George, though two low peaks occur in the 15-day range and at about 6.4 days; propagation speeds are slow. Between George and Port Elizabeth four relatively small peaks emerge, with associated wide ranges in speeds. Much higher coherences are found from Port Elizabeth eastwards.

Figure 10 shows time-lagged cross-correlations between winds at the various sites and sea level at East London and Port Elizabeth. As noted by Allen and Denbo (1984), in a strongly wind-forced region the variation in local sea level is generally more highly correlated with wind at locations in the direction from which CTWs would propagate. The gradient in the peak correlation is approximately the same in the two cases and gives a speed of about 7.5 m s^{-1}, within the rather wide ranges given in Table 2. Allen and Denbo (1984) showed that this speed (estimated from the wind–sea level correlation) should match that of the free CTWs. From Table 3, this falls in the range of calculated speeds for the south coast region (E, F, G and H) and agrees tolerably with the expected theoretical value of 8.0 cm s^{-1} (obtained by weighted inverse average), confirming that the sea level observations are consistent with the properties of wind-forced CTW theory.

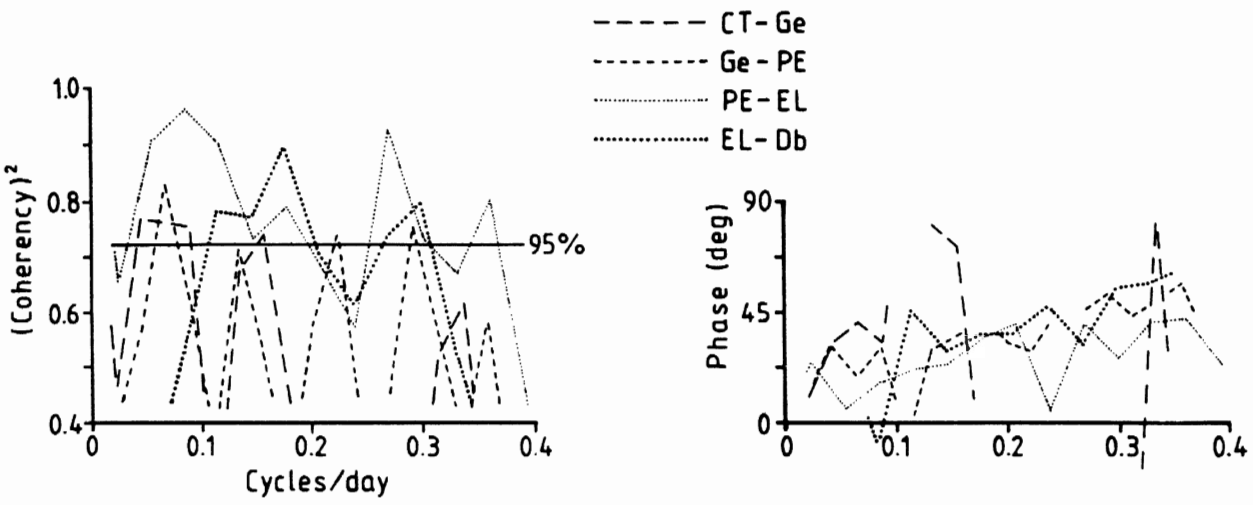

FIG. 9. Coherency squared and phase spectra of winds for adjacent sites. The 95% confidence limit is shown, with phase values also drawn only for higher values of coherency. The phase is positive if the first-mentioned site leads.

6. Discussion

The results presented here confirm that, along sections of the South African coast, large sea level events propagate in an anticlockwise sense around the subcontinent. Their characteristics have identified these as CTWs, although there are still some discrepancies between the theoretical structures and those emerging from the analysis of available data. In the east this may be related to the inability of the stratified model to account for changes due to the proximity of the Agulhas Current.

The results suggest that it is essentially along a relatively short section of the south and east coasts (about 700 km) that substantial amplitude CTWs occur, and it is these that will be specifically discussed here. Reasons for more limited CTW activity along the west coast may be the nature of the wind forcing and the topography. On the other hand, the influence of the Agulhas Current in damping out the waves on the east coast means that minimal activity is recorded at Durban (Brink 1990); it is from about Port Elizabeth northwards that the Current can be expected to exert a major effect on the CTWs (Goschen and Schumann 1990).

Estimates of the sea level propagation speed on the south coast show a good deal of scatter (Table 2). The ranges vary from 4.4 to 5 m s^{-1} on the western side of the Agulhas Bank, from 5 to a maximum of about 9 m s^{-1} for the central section, and decreasing to about 2.5 m s^{-1} in the east where the shelf is narrow and the Agulhas Current becomes important. The trend of these estimates follows the theoretical values of Table 3, but generally the observed speeds are slower than the model speeds. This is puzzling, because models which include both forced and free motions (e.g. Allen and Denbo 1984) show that the rate of sea level propagation ought to be faster than that of free waves. If the winds propagate alongshore in the same sense as the free CTWs, then it is less obvious what the speed of sea level propagation would be, although it seems intuitive that it would fall between the speed of wind propagation (7.4 m s^{-1} from Fig. 8) and the 8.0 m s^{-1} of theoretical free waves. This is marginally higher than the maximum observed CTW overall value of 6.5 m s^{-1} obtained from Fig. 5 and within the higher speed ranges of Table 2. The presence of higher mode (slower) CTWs (Chapman et al. 1988) would decrease the theoretical speeds, but this would then degrade the good model-observation phase speed agreement obtained from wind–sea level correlations.

The time-lagged correlations between sea level and wind (Fig. 10) agree well with Allen and Denbo (1984), who show that the maximum correlation should occur along a line having the same slope (7.5 m s^{-1}) as the free wave phase speed (8 m s^{-1}). The quality of this agreement makes it difficult to believe that higher modes have a substantial effect on sea level between Cape Town and Port Elizabeth. Indeed, dominance by the first mode would not be surprising because of the likely resonance associated with the near agreement in propagation speeds between free CTWs (8 m s^{-1}) and wind systems (7.4 m s^{-1}). Higher modes could nonetheless be present, since they are not expected to contribute greatly to coastal sea level fluctuations. In essence, it can be inferred that the response of the ocean is complex, and that a modal solution is only one way to approach the problem. Clarke and van Gorder (1986) considered the direct wind-forced and free response together, and such an analysis could also be useful here, given better wind data.

The results presented here have confirmed the presence of large amplitude CTWs along the South African south coast also suggested by de Cuevas et al. (1986) and Jury et al. (1989). The large CTWs described by Krause and Radok (1976) also occur on a zonal coast-

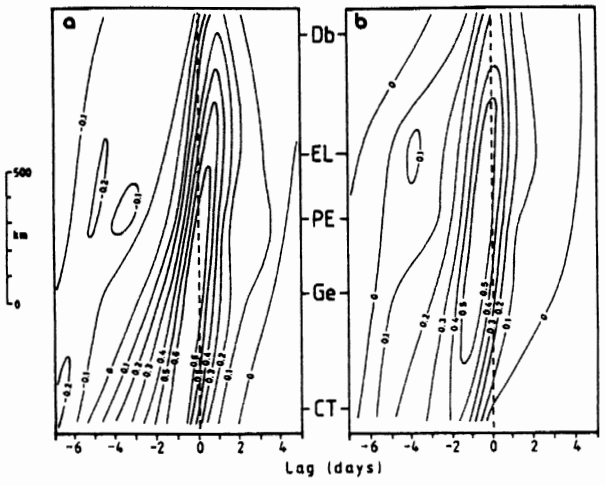

FIG. 10. Normalized time-lagged cross-correlations between winds at the various sites given on the ordinate axis, and sea level at (a) Port Elizabeth, and (b) East London.

line along Australia's south coast, possibly as a result of a similar near-resonance situation between winds and free wave speeds. They investigated the propagation of air pressure systems, but it may be that wind systems do not propagate at the same speed, as found by Schumann (1989) for the South African case; it is after all the winds which are expected to be the prime generating function.

The results presented here have not addressed seasonal variations, in particular changes in the wind field (Hunter 1987) and oceanic density structures (section 4). The time variation of sea level contours presented in Figs. 2 and 7 for the two intensive experimental periods give an indication of a marked 10-day fluctuation in April and May, but with a shorter period with smaller amplitudes dominant later in the year. Krause and Radok (1976) found marked peaks in sea level spectra at about 4.5 and 10 days for 1968 data, but with the September period having the greater amplitude. The results of de Cuevas et al. (1986) do not show any definite seasonal variations, so that at this stage it is not possible to identify positively whether such consistent longer-term periods exist. In some cases the marked peaks in sea level measured at East London are associated with particular weather events, e.g., during the three days 15 to 17 May a very deep low passed south of Africa, and was responsible for severe storm conditions along the south coast.

The results have shown the importance of CTWs in the dynamics of the coastal ocean around South Africa. In particular, the strong current reversals observed off East London during the passage of such a CTW are impressive testimony to the effect they can have. Schumann (1987) has already speculated on the importance such current reversals could have for the "sardine run"—an annual mass migration of sardines in a northeastward direction starting near Port Elizabeth and ending north of Durban. The changes in sea level—commonly more than 50 cm according to Table 1—can also have substantial effects along a coast where the spring tide amplitude can be 200 cm but the neap tide can be less than 50 cm.

Acknowledgments. The following organizations are thanked for data used in this analysis: The National Research Institute for Oceanology (now the Division of Earth, Marine and Atmospheric Science and Technology) of the CSIR for the East London ship, weather station and mooring data, the South African Hydrographic Office for sea level data, the Weather Bureau for air pressure and wind records from the various airports, and the Sea Fisheries Research Institute for the Hondeklip air pressure data. Fanie Strumpher and Judy Martin were responsible for the initial editing and processing of the data. KHB acknowledges support from the Office of Naval Research, Physical Oceanography (code 1122PO).

REFERENCES

Allen, J. S., and D. W. Denbo, 1984: Statistical characteristics of the large-scale response of coastal sea level to atmospheric forcing. *J. Phys. Oceanogr.*, **14**, 1079–1094.

Brink, K. H., 1990: On the damping of free coastal-trapped waves. *J Phys. Oceanogr.*, **20**, 1219–1225.

——, and D. C. Chapman, 1987: Programs for computing properties of coastal-trapped waves and wind-driven motions over the continental shelf and slope (second edition). Woods Hole Oceanographic Institution Tech. Rep., WHOI-87-24, 119 pp.

Brooks D. A., and C. N. K. Mooers, 1977: Wind-forced continental shelf waves in the Florida Current. *J. Geophys. Res.*, **82**, 2569–2576.

Chapman, D. C., 1987: Application of wind-forced, long, coastal-trapped wave theory along the California coast. *J. Geophys. Res.*, **92**, 1798–1816.

——, S. J. Lentz and K. H. Brink, 1988: A comparison of empirical and dynamical hindcasts of low-frequency, wind-driven motions over a continental shelf. *J. Geophys. Res.*, **93**, 12 409–12 422.

Clarke, A. J., and K. H. Brink, 1985: The response of stratified, frictional flow of shelf and slope waters to fluctuating large-scale, low-frequency wind forcing. *J. Phys. Oceanogr.*, **15**, 439–453.

——, and S. Van Gorder, 1986: A method for estimating wind-driven frictional, time-dependent, stratified shelf and slope water flow. *J. Phys. Oceanogr.*, **16**, 1013–1028.

de Cuevas, B. A., G. B. Brundrit and A. M. Shipley, 1986: Low-frequency sea-level fluctuations along the coasts of Namibia and South Africa. *Geophys. J. Roy. Astron. Soc.*, **87**, 33–42.

Freeland, H. J., F. M. Boland, J. A. Church, A. J. Clarke, A. M. G. Forbes, A. Huyer, R. L. Smith, R. O. R. Y. Thompson and N. J. White, 1986: The Australian Coastal Experiment: A search for coastal trapped waves. *J. Phys. Oceanogr.*, **16**, 1230–1249.

Gill, A. E., 1977: Coastally trapped waves in the atmosphere. *Quart. J. Roy. Meteor. Soc.*, **103**, 431–440.

——, and E. H. Schumann, 1979: Topographically induced changes in the structure of an inertial coastal jet: Application to the Agulhas Current. *J. Phys. Oceanogr.*, **9**, 975–991.

Goschen, W. S., and E. H. Schumann, 1990: Agulhas Current variability and inshore structures off the Cape Province, South Africa. *J. Geophys. Res.*, **95**, 667–678.

Halliwell, G. R., and J. S. Allen, 1984: Large-scale sea level response to atmospheric forcing along the west coast of North America, summer 1973. *J. Phys. Oceanogr.*, **14**, 864–886.

Halpern, D., and R. D. Pillsbury, 1976: Influence of surface waves on subsurface current measurements in shallow water. *Limnol. Oceanogr.*, **21**, 611–616.

Harris, T. F. W., 1978: Review of coastal currents in Southern African waters. South African National Scientific Programmes, Rep. No. **30,** CSIR, 103 pp.

Hunter, I. T., 1982: The coastal wind field of the southern Cape. *Proc. of the 18th Coastal Engineering Conf.*, ASCE, Cape Town, 2551–2561.

——, 1987: The weather of the Agulhas Bank and Cape south coast. CSIR Res. Rep. 634, 184 pp.

Jury, M., C. MacArthur, F. Shillington and C. Reason, 1989: Observations of trapped waves in the atmosphere and ocean along the coast of Southern Africa. *South African Geogr. J.*, submitted.

Krause, G., and R. Radok, 1976: Long waves on the Southern Ocean. *Waves in Water of Variable Depth*, D. G. Provis, R. Radok, Eds., Springer-Verlag, 221–231.

Kundu, P. K., and J. S. Allen, 1976: Some three-dimensional characteristics of low-frequency current fluctuations near the Oregon Coast. *J. Phys. Oceanogr.*, **6,** 181–199.

LeBlond, P. H., and L. A. Mysak, 1978: *Waves in the Ocean.* Elsevier, 602 pp.

Mitchum, G. T., and A. J. Clarke, 1986: The frictional nearshore response to forcing by synoptic scale winds. *J. Phys. Oceanogr.*, **16,** 934–946.

Nelson, G., and L. Hutchings, 1983: The Benguela upwelling area. *Progress in Oceanography*, Vol. 12, Pergamon, 333–356.

Pearce, A. F., 1977: Some features of the upper 500 m of the Agulhas Current. *J. Mar. Res.*, **35,** 731–753.

Preston-Whyte, R. A., and P. D. Tyson, 1973: Note on pressure oscillations over South Africa. *Mon. Wea. Rev.*, **101,** 650–659.

——, and ——, 1988: *The Atmosphere and Weather of Southern Africa.* Oxford University Press, 374 pp.

Schumann, E. H., 1982: Inshore circulation of the Agulhas Current off Natal. *J. Mar. Res.*, **40,** 43–55.

——, 1983: Long-period coastal trapped waves off the south-east coast of southern Africa. *Contin. Shelf Res.*, **2,** 97–107.

——, 1987: The coastal ocean off the east coast of South Africa. *Trans. Roy. Soc. South Africa*, **46,** 215–229.

——, 1989: The propagation of air pressure and wind systems along the South African coast. *South African J. Sci.*, **85,** 382–385.

——, and L.-A. Beekman, 1984: Ocean temperature structures on the Agulhas Bank. *Trans. Roy. Soc. South Africa*, **45,** 191–203.

Schwing, F. B., L.-Y. Oey and J. O. Blanton, 1985: Frictional response of continental shelf water to local wind forcing. *J. Phys. Oceanogr.*, **15,** 1733–1746.

——, —— and ——, 1988: Evidence for non-local forcing along the southeastern United States during a transitional wind regime. *J. Geophys. Res.*, **93,** 8221–8228.